https://doi.org/10.5194/egusphere-2024-907
Preprint. Discussion started: 24 May 2024

Technical note: On the ice microphysics of isolated thunderstorms and non-thunderstorms in southern China: A radar polarimetric perspective

Chuanhong Zhao[*1,2], Yijun Zhang[*1,3], Dong Zheng[4], Haoran Li[4], Sai Du[5], Xueyan Peng[2], Xiantong Liu[5], Pengguo Zhao[2], Jiafeng Zheng[2], Juan Shi[6]

[1]*Department of Atmospheric and Oceanic Sciences & Institute of Atmospheric Sciences, Fudan University, Shanghai, China*

[2]*School of Atmospheric Sciences, Chengdu University of Information Technology, Chengdu, China*

[3]*Shanghai Key Laboratory of Ocean-land-atmosphere Boundary Dynamics and Climate Change & Shanghai Frontiers Science Center of Atmosphere-Ocean Interaction, Fudan University, Shanghai, China*

[4]*State Key Laboratory of Severe Weather, Chinese Academy of Meteorological Sciences & Laboratory of Lightning Physics and Protection Engineering, Chinese Academy of Meteorological Sciences, Beijing, China*

[5]*Guangzhou Institute of Tropical and Marine Meteorology, Guangzhou, China*

[6]*Chengdu Meteorological Office, Chengdu, China*

Corresponding authors: Dr. Yijun Zhang & Dr. Chuanhong Zhao are the co-corresponding authors.

E-mail: zhangyijun@fudan.edu.cn; zch@cuit.edu.cn

https://doi.org/10.5194/egusphere-2024-907
Preprint. Discussion started: 24 May 2024

Abstract

The determination of whether a cloud will evolve into a thunderstorm is beneficial for understanding thunderstorm formation and important for ensuring the safety of society. However, a clear understanding of the microphysics in clouds for the occurrence of lightning activity has not been attained. Vast field observations and laboratory experiments indicate that graupel, which is rimed ice, is a vital hydrometeor for lightning generation, and is the foundation of riming electrification. In this study, polarimetric radar and lightning observations are used to compare the ice microphysics associated with graupel between 57 isolated thunderstorms and 39 isolated non-thunderstorms, and the differences in radar parameters are quantified. Our results for the occurrence of lightning activity in clouds showed the following results: 1) the maximum difference in graupel volume on the −10°C isotherm height between thunderstorms and non-thunderstorms reached approximately 7.6 km^3; 2) the graupel particles approached spherical shapes with a mean Z_{DR} value of 0.3 dB, which likely indicated heavily rimed graupel was present; and 3) 98.2% of thunderstorms were equipped with the Z_{DR} column, and the mean depth was ~2.5 km. Our study deepens our understanding of lighting physics and thunderstorm formation.

Short summary

Understanding lightning activity is important for meteorology and atmospheric chemistry. However, the occurrence of lightning activity in clouds is uncertain. This study quantified the difference between isolated thunderstorms and non-thunderstorms. Here we showed lightning activity was more likely to occur with more graupel volume and/or more riming. And a deeper Z_{DR} column was associated with lightning occurrence. This information can aid in a deeper understanding of lighting physics.

Keywords: thunderstorm; lightning; riming; cloud microphysics

1. Introduction

Thunderstorms are typically severe convection clouds. Lightning is not only a severe

https://doi.org/10.5194/egusphere-2024-907
Preprint. Discussion started: 24 May 2024

weather hazard produced by thunderstorms but also a clear signature to mark the thunderstorm formation (MacGorman and Rust, 1998). Understanding lightning activity (especially for the first lightning flash, indicating the start of lightning activity in a cloud) is important for understanding the meteorological processes, the formation of thunderstorms (Uman and Krider, 1989; Rosenfeld et al., 2008; Fan et al., 2018), and for investigating related atmospheric chemistry, such as the formation of ozone and the primary oxidant in the troposphere, the hydroxyl radical (Pickering et al., 2016; Brune et al., 2021).

The determination of whether a cloud will evolve into a thunderstorm is very difficult. The occurrence of lightning activity in clouds is a complex process involving dynamics, microphysics and electrical processes (e.g., Krehbiel et al., 1979; MacGorman and Rust, 1998; Carey and Rutledge, 2000; Stolzenburg et al., 2001; Saunders, 2008; Zhang et al., 2009; Lang and Rutledge, 2011; Zhang et al., 2016; Stough and Carey, 2020; Lyu et al., 2023). Moreover, lightning shows different types depends on different environments (Uman and Krider, 1989; Boggs et al., 2022), intracloud lightning, cloud-to-ground lightning, cloud-to-cloud and cloud-to-air discharges. Some studies indicated the majority of the first lightning flashes are intracloud lightning, which was concluded from the statistical results observed by polarimetric radar and lightning location systems (e.g., Mattos et al., 2017; Zhao et al., 2021a). And there is a generally accepted electrification cause, especially for clarifying the first lightning flash occurrence correctly: noninductive charging (NIC) of two ice particles of different sizes during rebounding collisions in the presence of supercooled droplets, with the smaller ice particle being the ice crystal and the larger ice particle being the graupel (Takahashi, 1978; Latham, 1981; Saunders et al., 1991; MacGorman and Rust, 1998; Carey and Rutledge, 2000; Zhang et al., 2009; Takahashi et al., 2017, 2019; Qie et al., 2021; Lyu et al., 2023).

The NIC was proposed based on cold-chamber laboratory experiments (Reynolds et al., 1957; Takahashi, 1978); subsequently, field observations demonstrated that lightning production is critically linked to ice processes (i.e., graupel signatures) (Dye et al., 1986; Takahashi et al., 1999; Carey and Rutledge, 2000; Basarab et al., 2015; Stolzenburg et al., 2015; Mattos et al., 2016, 2017; Takahashi et al., 2017, 2019; Hayashi et al., 2021; Zhao et al., 2022). Therefore, graupel is a vital precipitation particle for riming electrification mechanism.

https://doi.org/10.5194/egusphere-2024-907
Preprint. Discussion started: 24 May 2024

Graupel is rimed precipitation ice. But the mechanisms for graupel formation will vary with cloud types. One pathway to graupel that is very common in warm based clouds worldwide is the development of rain drops in warm rain collision-coalescence processes, followed by lofting of the rain drop in the updraft to the supercooled temperature (which is frequently observed by polarimetric radar, called the differential reflectivity (Z_{DR}) column), then by drop freezing and finally riming into graupel or small hail. This coalescence-freezing mechanism is often the most important pathway to the first graupel/hail, the first significant electrification and the first lightning flash in warm based clouds (e.g., Brahams, 1986; Beard, 1992; Herzegh and Jameson, 1992; Bringi et al., 1997; Smith et al., 1999; Carey and Rutledge, 2000; Stolzenburg et al., 2015; Mattos et al., 2017). Another pathway to graupel or small hail production is initiated via the aggregation of ice crystals into snow aggregates, followed by riming of the snow aggregate into graupel and possibly even small hail as the rime density increases (Heymsfield, 1982; Li et al., 2018).

It should also be emphasized that the formation of graupel is closely related to not only the lightning activity but also the strength of updraft in clouds, the latent heat of freezing enhances updrafts, promoting severe storm formation (Rosenfeld, 1999; Zhang et al., 2004; Rosenfeld et al., 2008). More droplets freeze aloft and release more latent heat for nucleation, thereby invigorating convective updrafts and producing lightning, and deep convective clouds form (Rosenfeld, 1999; Zhang et al., 2004; Rosenfeld et al., 2008). Therefore, investigating the ice microphysics associated with graupel is essential for understanding the thunderstorm formation.

Polarimetric radar is a better observation system for tracking the specific location and timing of a cloud and inferring the microphysical characteristics within clouds (e.g., Seliga and Bringi, 1976; Zrnic and Ryzhkov, 1999; Kumjian, 2013; Hu et al., 2019; Huang et al., 2023). Many studies (e.g., Laksen and Stansbury, 1974; Marshall and Radhakant, 1978; Dye et al., 1986; Vincent et al., 2003; Woodard et al., 2012; Mattos et al., 2016, 2017; Hayashi et al., 2021; Zhao et al., 2022) have investigated the relationship between ice microphysics and lightning activity, and provided methods to predict the first lightning flash occurrence based on the riming electrification mechanism; specifically, the graupel-related reflectivity at −10°C or colder is a commonly supported leading reflectivity parameter in forecasting the first lightning flash.

https://doi.org/10.5194/egusphere-2024-907
Preprint. Discussion started: 24 May 2024

However, the performances of these methods vary with seasons, geography, or other atmospheric variables; more directly, different ice microphysics within different clouds dominate. There is no doubt that the graupel signatures inferred by polarimetric radar universally present in convective clouds, while some clouds involve no lightning (e.g., Woodard et al., 2012; Hayashi et al., 2021; Cui et al., 2022; Zhao et al., 2022). Specifically, the graupel signature inferred by polarimetric radar needs to be partitioned into more details according to the radar parameters. Therefore, we hope to better understand the ice microphysics associated with graupel within thunderstorms in this study.

We accomplish this goal by comparing the ice microphysics associated with graupel between isolated thunderstorms and non-thunderstorms during the warm season over southern China and quantifying differences of graupel magnitude and shape (implying the riming efficiency) in radar parameters, instead of studying the evolution variation within the same thunderstorm (the role of some polarimetric signatures would be covered in the same cloud evolution). To the best of our knowledge, no other study addressing this topic has been published yet. In addition, we explore the role of the coalescence-freezing mechanism in the production of lightning based on the information provided by the Z_{DR} column, a narrow vertical extension of positive Z_{DR} values above the 0°C isothermal height associated with updrafts and supercooled liquid water in deep moist convective storms (e.g., Hall et al., 1980; Ryzhkov et al., 1994; Kumjian and Ryzhkov, 2008; Kumjian, 2013; Kumjian et al., 2014; Snyder et al., 2015; Zhao et al., 2020; Chen et al., 2023). Isolated thunderstorms are common in southern China during warm season (Mai and Du, 2022). From the perspective of isolated storms in warm season, the physical processes within clouds will be easier to explain and the characteristics of graupel microphysics could be compared with that in cold based clouds (results in Li et al., 2018).

2. Materials and methods

In this study, 57/39 isolated thunderstorm/non-thunderstorm cells that occurred over South China in the warm seasons (from late May to early September) of 2016 and 2017 were analysed; the dataset used was the same as that used in Zhao et al. 2021a, 2022. The Guangzhou S-pol radar provided the radar data. The beam width of the S-pol radar was ≤1°, and a full radar volume scan lasted 6 minutes; this consisted of nine elevation angles with a radial resolution of 250 m. A

https://doi.org/10.5194/egusphere-2024-907
Preprint. Discussion started: 24 May 2024

quality control procedure was carried out to remove the ground clutter, anomalous propagation, and biological scatter, and the Z_{DR} offset of the raw data was corrected (Zhao et al., 2022). The quality-controlled radar data were interpolated onto a Cartesian grid at a horizontal resolution of 250 m and a vertical resolution of 500 m over 0.5 to 20 km above the mean sea level using nearest neighbour and vertical linear interpolation.

A hydrometeor identification method, based on the fuzzy logic algorithm, was carried out to discriminate the graupel particles, as in Zhao et al. (2021b). The algorithm and approximate ranges of the S-band values of each polarimetric variable essentially followed Park et al. (2009) and Kumjian (2013) with an improvement in the parameters in the membership functions of the fuzzy logic algorithm for the performance of the Guangzhou S-pol radar, especially for dry/wet snow particles (Wu et al., 2018). In addition, temperature information was added as one of a few factors to the hydrometeor identification method because it could separate the liquid precipitation from the solid hydrometeors to avoid visible identification errors (e.g., Bechini and Chandrasekar, 2015; Kouketsu et al., 2015; Zhao et al., 2020).

Three independent lightning location systems provided lightning observations. The low-frequency E-field detection array (LFEDA) can detect three-dimensional structures of intracloud lightning and/or cloud-to-ground lightning. The detection efficiency and mean location error of LFEDA for triggered lightning were approximately 100% and 102 m, respectively (Shi et al., 2017; Fan et al., 2018). The Earth Networks Lightning Location System (ENLLS) can detect two-dimensional locations for intracloud lightning and/or cloud-to-ground lightning. The detection efficiency and mean location error of the ENLLS for triggered lightning and the natural strike of tall structure lightning were approximately 77% and 685 m, respectively (Zheng et al., 2017). The Guangdong Lightning Location System (GDLLS) can locate cloud-to-ground lightning. The detection efficiency and mean location error of the GDLLS for triggered lightning and the natural strike of tall structure lightning were approximately 94% and 741 m, respectively (Chen et al., 2012).

Three lightning location systems were used to more accurately detect the first lightning flashes within clouds. The lightning flash was assigned to its corresponding cell by using the boundary of the cell as a constraint every 6 minutes. The first lightning flash of a thunderstorm

https://doi.org/10.5194/egusphere-2024-907
Preprint. Discussion started: 24 May 2024

was defined by its first detection from one of three lightning location systems. An isolated non-thunderstorm cell was selected when no flash in the cell was detected by any of the three lightning location systems. To ensure detection-data quality, the analysis area was restricted to the regions of overlapping coverage between the S-pol radar radius of 25-100 km and the LFEDA station network centre radius of 70 km, as in Zhao et al. (2021a, 2022). Any isolated cell storm generated within the analysis area that moved completely outside the analysis area or merged with other precipitation cells was excluded. The intersection of the 20 dBZ contours of the two intersected cells is referred to as merging. For thunderstorms, we ensure that the first lightning flash of the cell must occur before merging or when there is no merging. For storm cell development, if no merging process occurs and the maximum reflectivity of this cell starts to fade with a value of less than 30 dBZ later, the evolutionary process of a cell will mark the cessation stage. Our objective is to focus on isolated storm cell; therefore, if merging process occurs before the fading of the maximum reflectivity of this cell, the evolutionary process of the cell will also signal the cessation stage.

In the dataset, six merging events occurred in non-thunderstorms, and the values of maximum reflectivity for these non-thunderstorms did not increase after merging occurred. In addition, the maximum reflectivity within any non-thunderstorm cell from initiation to cessation must exceed 45 dBZ to avoid the statistics of weak precipitation cells. Non-thunderstorms are characterized by no flash occurrence from initiation to cessation. The sounding data were obtained from the Qingyuan meteorological observatory, which also provided the environmental temperature. Isolated thunderstorm/non-thunderstorm cells were identified and tracked manually based on the observations from the S-pol radar and lightning location systems. The average distances between these storms and the radar/sounding site were approximately 70 and 56 km, respectively. More details related to these data and the selection methods for isolated thunderstorm and non-thunderstorm cells are available in Zhao et al. (2021a, 2022).

In this study, the evolution cycle of a thunderstorm contains three stages: (i) the first radar volume scanning in cases where $Z_H \geq 5$ dBZ is called the first stage (hereafter referred to as the #1 stage), (ii) the intermediate radar volume scanning between the first stage and the third stage is called the second stage (hereafter referred to as the #2 stage), and (iii) the radar volume scanning

https://doi.org/10.5194/egusphere-2024-907
Preprint. Discussion started: 24 May 2024

in cases where the first lightning flash occurs is called the third stage (hereafter referred to as the #3 stage). Similarly, the evolution cycle of a non-thunderstorm also contains three stages, but radar volume scanning in cases where the most intense echo occurs is called the third stage; here, the most intense echo is used to indicate the strongest convection development stage of non-thunderstorms for comparison with the first lightning flash stage of thunderstorms. The average durations from the first stage to the third stage for thunderstorms and non-thunderstorms are 19 and 24 minutes, respectively. The majority of first lightning flash events (~98%) are considered to be intracloud flashes, and only one is considered to be cloud-to-ground flash. The majority of first lightning flashes (~91%) are determined by the LFEDA due to its superior detection efficiency and accuracy for lightning flashes in this analysis area.

3. Results

3.1 Morphology and intensity of the echoes in and/or before the first lightning flash occurrence

The orange scatters and grey triangles with error bars in Figure 1a describe the echo-top heights and echo-base heights of the 57 thunderstorms and 39 non-thunderstorms from the first stage to the third stage of cloud development using the reflectivity threshold (0 dBZ), and the echo depths are shown in the box plots. The echo-top heights of thunderstorms or non-thunderstorms increase as clouds develop. For the echo-top height data, approximately 95% of the thunderstorms exceeded the −30°C isotherm height, and 85% exceeded the −38°C isotherm height of the glaciated layer during the third stage of cloud development; however, only 26% and 23% of non-thunderstorms exceeded the −30°C and the −38°C isotherm heights, respectively, during the third stage of cloud development. However, the echo-base heights mildly decreased with the development of clouds; slight differences in the echo-base heights occurred between thunderstorms and non-thunderstorms. Deep convective clouds, indicated by thunderstorms, were formed when first lightning flashes occurred; approximately 84% of thunderstorms and only 23% of non-thunderstorms achieved an echo depth of 10 km.

Figure 1b shows that the differences in the mean (maximum) values of the Z_H between the thunderstorm and non-thunderstorm periods during each stage are slight. Thunderstorms exhibit

https://doi.org/10.5194/egusphere-2024-907
Preprint. Discussion started: 24 May 2024

greater Z_H intensities than non-thunderstorms, except for those in the first stage of cloud development. The signature of larger mean or maximum values of Z_H in non-thunderstorms during the first stage than in thunderstorms has been discussed by Zhao et al. (2022), and this aspect is not the focus of this study. The mean or maximum values of Z_H in thunderstorms increase and exceed those in non-thunderstorms when first lightning flashes occur; however, the box plots show that we cannot effectively differentiate the thunderstorms from the non-thunderstorms with respect to the Z_H intensity.

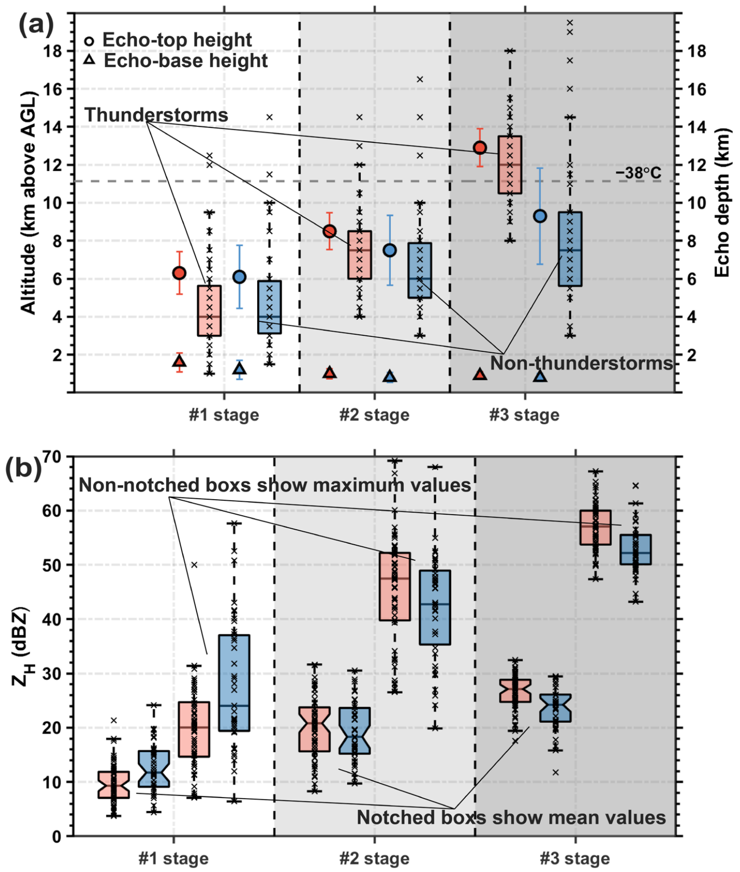

Figure 1. Characteristics of radar echoes with cloud development. (a) Echo-top heights of 0 dBZ and echo-base heights of 0 dBZ for 57 thunderstorm and 39 non-thunderstorm cells from the first stage to the third stage of cloud development indicated by scatter points and triangles, respectively, with error bars. Error bars are computed as 95% confidence intervals. Box plots for the 57 thunderstorms (orange) and 39 non-thunderstorms (blue) for echo depths; all units are in km. The dashed grey lines indicate the

https://doi.org/10.5194/egusphere-2024-907
Preprint. Discussion started: 24 May 2024

−38°C and 0°C isotherm heights, respectively. (b) The mean (maximum) value of the Z_H in a thunderstorm or a non-thunderstorm during every stage is shown in notched box plots (non-notched box plots), with all units in the dBZ. The median values in the box plots are shown as black horizontal continuous lines. The temperature data were obtained from the sounding data of the Qingyuan meteorological observatory.

3.2 Variation in the graupel magnitude with cloud development

Graupel is a vital precipitation particle for riming electrification mechanism, and its radar signature is not obscured by small ice particles. In contrast, the radar signature of small ice particles (i.e., ice crystals) tends to be obscured by large ice particles (e.g., graupel). Thus, to investigate the microphysical characteristics related to the first lightning flash occurrence during storms, we obtained inferred "graupel", which was derived from the fuzzy-logic method based on S-pol radar (Park et al., 2009; Kumjian, 2013; Zhao et al., 2021b, 2022).

Each histogram in Figure 2 indicates the mean value of the volume (the volume is computed by the radar sample grid; each grid is 0.03125 km^3, 0.25 km × 0.25 km × 0.5 km), which corresponds to the total graupel in total graupel on a height layer for 57 thunderstorms or 39 non-thunderstorms during each stage of cloud development. Graupel is rare in thunderstorms or non-thunderstorms during the first stage of cloud development (e.g., Dye et al., 1986; Mattos et al., 2017), and only 5% (13%) of thunderstorms (non-thunderstorms) show graupel signals (Figure 2). With the development of clouds, that ratio in thunderstorms (non-thunderstorms) is reached 79% (51%) and 100% (95%) during the second and third stages of cloud development, respectively.

https://doi.org/10.5194/egusphere-2024-907
Preprint. Discussion started: 24 May 2024

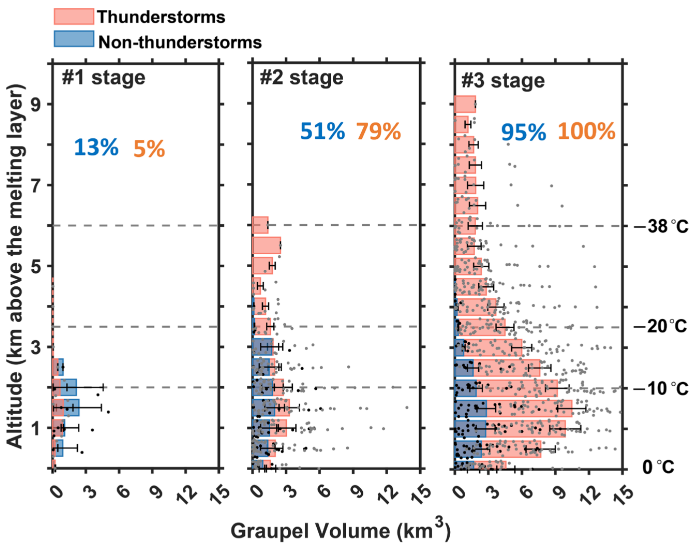

Figure 2. Distribution of the graupel signals and volume with cloud development. Histogram plots with error bars for the distribution of the graupel volume above the melting layer for thunderstorm and non-thunderstorm cells during each stage of cloud development. Each grey dot indicates the total graupel volume on a height layer of a thunderstorm; the black dots indicate non-thunderstorm units in km^3. The mean graupel volume in a height layer for the 57 thunderstorms is displayed as an orange histogram and a blue histogram shows the graupel volume for non-thunderstorm (in km^3). Error bars are computed as 95% confidence intervals. The numerical values in orange and blue are the percentages of thunderstorms and non-thunderstorms that show the graupel signals, respectively. The left column is for the first stage of cloud development, and the right and middle rows are for the third and second stages of cloud development, respectively. In addition, the values are given by bilateral box plots. The −10°C, −20°C, and −38°C isotherm heights are displayed in the histogram plots.

The greatest difference in the graupel magnitude between thunderstorms and non-thunderstorms is found during the third stage of cloud development; the maximum difference in the graupel volume in a height layer reaches approximately 7.6 km^3, and the height of the maximum difference is near the −10°C isotherm height. To note, the graupel volume should be more accurately phrased as the presence of graupel in this volume These characteristics indicate that graupel signals are universally present in thunderstorms and non-thunderstorms, and the difference in the magnitude of the graupel volume is the key for the first lightning flash occurrence.

3.3 More microphysical information based on radar variables

As the graupel volume increases from the first radar track to the occurrence of the first

https://doi.org/10.5194/egusphere-2024-907
Preprint. Discussion started: 24 May 2024

lightning flash, the graupel volume in thunderstorms is clearly greater than that in non-thunderstorms during the third stage of cloud development. However, the understanding of the details of the increase in the graupel volume is limited (e.g., the variation in the maximum dimension or number concentration and precursor signature). In addition, although the coalescence-freezing mechanism dominating the formation of graupel within warm-season thunderstorms is generally accepted (e.g., Brahams, 1986; Beard, 1992; Herzegh and Jameson, 1992; Bringi et al., 1997; Smith et al., 1999; Carey and Rutledge, 2000; Stolzenburg et al., 2015; Mattos et al., 2017), more studies are needed to support this mechanism.

The Z_{DR} parameter could provide more information on the graupel (e.g., shape) and supercooled liquid water (e.g., Z_{DR} column). The variance in the shape of the graupel indicates the riming efficiency; specifically, the heavily rimed ice particles approach a spherical shape. Although the shape cannot directly indicate the variation in the maximum dimension, the speculated riming efficiency from the variation in the graupel shape could provide related information on the maximum dimension of graupel particles; typically, more spherical (a decrease in Z_{DR}) and more riming result in a stronger Z_H corresponding to a larger maximum dimension. The supercooled liquid water indicated by positive Z_{DR} values above the 0°C isothermal height is the precursor for freezing particles, followed by the embryo of graupel particles. Thus, the existence and/or variance of the Z_{DR} column before the occurrence of the first lighting flash could support the coalescence-freezing mechanism. Moreover, we can obtain the quantitative difference in the Z_{DR} between thunderstorms and non-thunderstorms, especially for the occurrence of the first lightning flash.

a. Differences in the shapes of the graupel particles between thunderstorms and non-thunderstorms

Figure 3 shows the average intensities of the Z_H and Z_{DR} with error bars corresponding to the graupel particles above the ~−3°C isotherm height (avoiding melting effects) in thunderstorms and non-thunderstorms during each stage of cloud development. Based on the results, the average intensity of the Z_{DR} corresponding to the graupel particles decreases with cloud development, which indicates that the graupel particles gradually approach a spherical shape (Figure 3d); the most remarkable indicator is that the graupel particles in the majority of thunderstorms have lower

https://doi.org/10.5194/egusphere-2024-907
Preprint. Discussion started: 24 May 2024

Z_{DR} values with a mean value of ~0.3 dB when first lightning flashes occur; however, this lower Z_{DR} value is not evident in non-thunderstorms, even during the most intense echo stage of cloud development, with a the mean value of ~0.5 dB). Moreover, the Z_{DR} values approach 0 dB, corresponding to stronger Z_H values when the average intensity of the Z_H exceeds 35 dBZ. Thus, we speculated that heavily rimed graupel was present, the size increased, and the shape tended to be spherical.

Li et al. (2018) presented a quantitative relationship between the riming and shape of snow aggregates in only winter snowstorms; however, we examined the relationship in deep convection or thunderstorms in present study. In Li et al. (2018), particles with $Z_H > 15$ dBZ, $Z_{DR} > 0.4$ dB, and above the ~−3°C isotherm height are likely to be lightly rimed (rime mass fraction ~< 0.2), and particles with $Z_H > 15$ dBZ, $-0.2 < Z_{DR} < 0.15$ dB, and above the ~−3°C isotherm height are likely to be moderately or heavily rimed (rime mass fraction ~> 0.4). The rime mass fraction is defined as the ratio of the accreted ice mass to the total ice particle mass; more details on the rime mass fraction can be found in Li et al. (2018). In Figures 3a, b, and c, the shaded area in blue indicates the high possibility that graupel particles are lightly rimed, comparatively, the shaded area in yellow indicates that the graupel particles are moderately or heavily rimed, as in Li et al. (2018). The results from Li et al. (2018) are limited to only winter snowstorms; the mechanism for producing graupel in winter snowstorms is different from that in warm-season thunderstorms, but the final shape of the graupel particles when first lightning flashes occur in this study approaches the shape of moderately or heavily rimed ice particles in Li et al. (2018).

https://doi.org/10.5194/egusphere-2024-907
Preprint. Discussion started: 24 May 2024

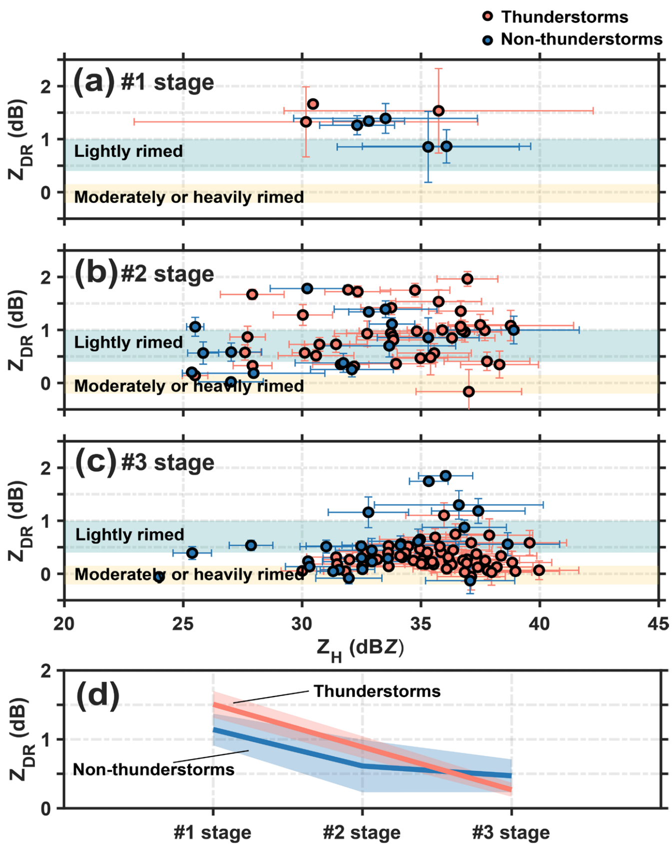

Figure 3. Graupel shape in and/or before the first lightning flash occurrence. Scatter plots with error bars for the mean values of Z_H and Z_{DR} corresponding to graupel particles above the ~−3°C isotherm height in thunderstorm (orange) and non-thunderstorm (blue) cells during each stage of cloud development. Error bars are computed as 95% confidence intervals. The inferred differences in the efficiency of the riming process are shown by the threshold values of Z_H and Z_{DR}; the shaded area in blue indicates the high possibility that graupel particles are lightly rimed, and comparatively, the shaded area in yellow indicates that graupel particles are moderately or heavily rimed. (a) First stage, (b) second stage, and (c) third stage of cloud development. In addition, the statistical mean values are given in (d), and the orange (blue) line indicates the mean value of the Z_{DR} corresponding to the above scatters in thunderstorms (non-thunderstorms) during each stage of cloud development. The shaded area indicates the 95% confidence interval.

b. Signature of the Z_{DR} column

Previous studies utilized Z_{DR} values ranging from 0.5 to 5 dB within the strong reflectivity range (35~50 dBZ) above the melting layer to describe the area of the Z_{DR} column (e.g., Illingworth et al., 1987; Tuttle et al., 1989; Ryzhkov et al., 1994; Scharfenberg et al., 2005; Woodard et al., 2012; Kumjian et al., 2014; Snyder et al., 2015; Zhao et al., 2020). Since the

https://doi.org/10.5194/egusphere-2024-907
Preprint. Discussion started: 24 May 2024

development of these clouds in this study occurred during the early stage of the full evolution cycle of thunderstorms, the size of the supercooled liquid water drop would not be large. Thus, we used Z_{DR} values of 0.5 dB within a reflectivity range of 30 dBZ above the melting layer to investigate the characteristics of the Z_{DR} column.

Figure 4 shows the height of the Z_{DR} column within thunderstorms or non-thunderstorms during each stage of cloud development. The computation of the Z_{DR} column height is similar to that in Snyder et al. (2015), and this height is the vertically continuous maximum depth of the Z_{DR} column. The signature of the Z_{DR} column clearly coincides with the development of clouds (Figure 4). Most thunderstorms (98.2%) displayed a deep Z_{DR} column with a mean depth of the Z_{DR} column of ~2.5 km when the first lightning flash occurred; however, only 48.7% of non-thunderstorms corresponded to a shallow Z_{DR} column with a mean value of ~1.1 km (Figure 4a, b). Moreover, 66.7% of the thunderstorms exhibited a deeper Z_{DR} column with a mean value of ~1.5 km during the second stage of cloud development, and 30.8% of non-thunderstorms showed a shallower Z_{DR} column with a mean value of ~0.99 km during the second stage of cloud development (Figure 4a, b). However, the occurrence frequency of the Z_{DR} column for non-thunderstorms is slightly greater than that for thunderstorms during the first stage of cloud development (Figure 4a, b). However, this phenomenon may be related to the results from Zhao et al. (2022); specifically, the Z_{DR} values below the −10°C isotherm height of non-thunderstorms were greater than those of thunderstorms within the first radar echo.

https://doi.org/10.5194/egusphere-2024-907
Preprint. Discussion started: 24 May 2024

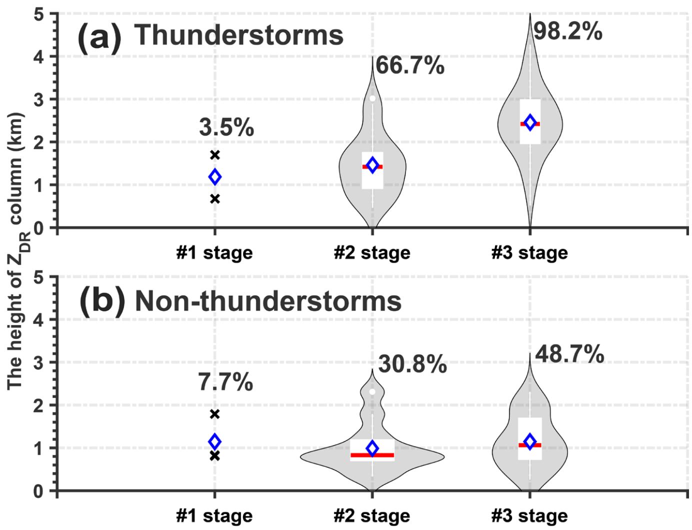

Figure 4. **Z_{DR} column information in and/or before the first lightning flash occurrence.** Violin plots of the Z_{DR} column depth of thunderstorm or non-thunderstorm cells during each stage of the cloud development, showing the average (blue diamond), interquartile range (rectangle), 10th and 90th percentiles (whiskers), and kernel density estimation (grey shading). (a) Thunderstorms. (b) Non-thunderstorms. The numerical value is the percentage of thunderstorms that show the Z_{DR} column signature.

4. Summary

In this study, the combination of a lightning location system and dual-polarization radar measurements was employed to study the ice microphysics of isolated thunderstorms and non-thunderstorms in southern China during warm season. From a unique perspective of comparing the radar signatures and inferred graupel information between the isolated thunderstorm and non-thunderstorm cells during each stage of cloud development, the lightning generation in clouds was found to be good indicator of the formation of deep convective clouds. The echo intensities, echo-top heights and echo depths were greater in clouds when the first lightning flash occurred, which indicated more severe updrafts in thunderstorms than in non-thunderstorms. Moreover, a greater graupel volume were clearly observed in clouds when the first lightning flash occurred, and the maximum difference in graupel volume in the height layer between thunderstorms and non-thunderstorms reached approximately 7.6 km^3, corresponding to an approximate −10°C isotherm height.

The variation in the average Z_{DR} intensity corresponding to the graupel particles above the

https://doi.org/10.5194/egusphere-2024-907
Preprint. Discussion started: 24 May 2024

~−3°C isotherm height during the three stages of cloud development indicated that graupel particles were more spherical (the mean Z_{DR} value was ~0.3 dB) and were more likely to generate lightning. The Z_{DR} values approached 0 dB, corresponding to stronger Z_H values; the average intensity of the Z_H exceeded 35 dBZ. When the first lightning flashes occurred in clouds, a decrease in the Z_{DR} value and an increase in the Z_H value of graupel were observed; these results indicate that heavily rimed ice particles were present, and the shape of these particles was similar to that of moderately or heavily rimed ice particles within winter snowstorms.

Moreover, the results indicated that the highly related relationship between the Z_{DR} column and the occurrence of the first lightning flash was present, 98.2% of the clouds were equipped with a Z_{DR} column with a mean depth of ~2.5 km when the first lightning flash occurred. In addition, a deeper Z_{DR} column corresponded to a greater graupel volume. Thus, the coalescence-freezing mechanism dominated the formation of graupel within warm-season isolated thunderstorms over southern China, the results were consistent with those of previous studies (e.g., Brahams, 1986; Beard, 1992; Herzegh and Jameson, 1992; Bringi et al., 1997; Smith et al., 1999; Carey and Rutledge, 2000; Stolzenburg et al., 2015; Mattos et al., 2017), but increasing the knowledge about quantified characteristics of Z_{DR} column for the first lightning flash occurrence in warm-season isolated thunderstorms based on relatively large sample statistics (Table 1 shows details of cases in related investigations for isolated thunderstorms).

References	Number of cases (thunderstorms)	Number of cases (non-thunderstorms)
Workman and Reynolds, 1949	12	×
Reynolds and Brook, 1956	5	×
Goodman et al., 1988	1	×
Ramachandran et al., 1996	2	×
Jameson et al., 1996	3	×
Woodard et al., 2012	31	19
Stolzenburg et al., 2015	3	×
Mattos et al., 2017	46	×

Table 1. Details of cases in references.

However, our results were obtained by comparing the characteristics of polarimetric parameters according to the graupel particles inferred by a hydrometeor identification method. The

https://doi.org/10.5194/egusphere-2024-907
Preprint. Discussion started: 24 May 2024

inferred graupel volume was an indication that graupel could be present among other hydrometeors in that volume. From the perspective of radar, the dominant particle in this volume was graupel. Fortunately, we focused on comparing the graupel volume between the thunderstorms and non-thunderstorms; therefore, we believe that the errors in this volume resulting from other secondary hydrometeors could be neutralized by the comparison with the same detected data and methods. In addition, although the results from this study could provide a possible index or method based on polarimetric radar for warning of the first lightning flash occurrence within the warm-season cell storms, understanding the microphysical characteristics and applying that in the numerical simulations would be the optimal method to provide lightning flash warnings in the future.

Acknowledgements

The authors acknowledge the Guangzhou Institute of Tropical and Marine Meteorology for collecting and archiving the radar, the surface, and the lightning observations. And authors also acknowledge the State Key Laboratory of Severe Weather, Chinese Academy of Meteorological Sciences & Laboratory of Lightning Physics and Protection Engineering for three-dimensional lightning location data. This research has been supported by the National Natural Science Foundation of China (grants 42175090, 42305079, 42305087), the China Postdoctoral Science Foundation (grant 2023M730619), the Scientific Research Fund of Chengdu University of Information Technology (grants KYTZ202213, KYQN202301, KYQN202307), the Scientific Research Fund of CAMS State Key Laboratory of Severe Weather (2021LASW-B02), and Basic Research Fund of CAMS (451490, 2023Z008).

Open Research

The sounding data is available at http://weather.uwyo.edu/upperair/sounding.html. The data in this study can be obtained from Figshare (Zhao, 2024).

https://doi.org/10.5194/egusphere-2024-907
Preprint. Discussion started: 24 May 2024

References

Basarab, B. M., Rutledge, S. A., and Fuchs, B. R.: An improved lightning flash rate parameterization developed from Colorado DC3 thunderstorm data for use in cloud-resolving chemical transport models, *Journal of Geophysical Research: Atmospheres*, 120, 9481–9499, doi:10.1002/2015JD023470, 2015.

Beard, K. V.: Ice initiation in warm-base convective clouds: An assessment of microphysical mechanisms, *Atmospheric Research*, 28, 125–152, https://doi.org/10.1016/0169-8095(92)90024-5, 1992.

Bechini, R., and Chandrasekar, V.: A Semisupervised Robust Hydrometeor Classification Method for Dual-Polarization Radar Applications, *Journal of Atmospheric and Oceanic Technology*, 32, 22–47, https://doi.org/10.1175/JTECH-D-14-00097.1, 2015.

Boggs, L. D., Mach, D., Bruning, E., Liu, N., van der Velde, O. A., Montanyá, J., Cummer, S., Palivec, K., Chmielewski, V., MacGorman, D., and Peterson, M.: Upward propagation of gigantic jets revealed by 3D radio and optical mapping, *Science Advances*, 8, eabl8731, doi: 10.1126/sciadv.abl8731, 2022.

Braham, R. R. Jr.: The cloud physics of weather modification. Part 1: Scientific basis, *WMO Bulletin*, 35, 215–221, 1986.

Bringi, V. N., Knupp, K., Detwiler, A., Liu, L., Caylor, I. J., and Black, R. A.: Evolution of a Florida Thunderstorm during the Convection and Precipitation/Electrification Experiment: The Case of 9 August 1991, *Monthly Weather Review*, 125, 2131–2160, doi: https://doi.org/10.1175/1520-0493(1997)125<2131:EOAFTD>2.0.CO;2,1997.

Brune, W. H., McFarland, P. J., Bruning, E., Waugh, S., MacGorman, D., Miller, D. O., Jenkins, J. M., Ren, X., Mao, J., and Peischl, J.: Extreme oxidant amounts produced by lightning in storm clouds, *Science*, 372, 711–715, doi: 10.1126/science.abg0492, 2021.

Carey, L. D., and Rutledge, S. A.: The Relationship between precipitation and lightning in tropical island convection: A C-Band polarimetric radar study, *Monthly Weather Review*, 128, 2687–2710, https://doi.org/10.1175/1520-0493(2000)128<2687:TRBPAL>2.0.CO;2, 2000.

Chen, G., Zhao, K., Wen, L., Yang, J., Zheng, Y., Xu, F., Lyu, F., Sun, K., and Sun, L.: Linking ice-phase microphysics to raindrop characteristics in deep convection: A warm-sector extreme rainfall case study in Eastern China, *Earth and Space Science*, 10, e2022EA002697, https://doi.org/10.1029/2022EA002697, 2023.

Chen, L., Zhang, Y. J., Lyu, W., Zheng, D., Zhang, Y., Chen, S., and Huang, Z.: Performance evaluation for a lightning location system based on observations of artificially triggered lightning and natural lightning flashes, *Journal of Atmospheric and Oceanic Technology*, 29, 1835–1844, https://doi.org/10.1175/JTECH-D-12-00028.1, 2012.

Cui, Y., Zheng, D., Zhang, Y. J., Ruan, Z., Li, F., Yao, W., Meng, Q., and Zhao, C.: Association of lightning occurrence with precipitation cloud column structure at a fixed position, *Atmospheric Research*, 267, 105989, https://doi.org/10.1016/j.atmosres.2021.105989, 2022.

Dye, J. E., Jones, J. J., Winn, W. P., Cerni, T. A., Gardiner, B., Lamb, D., Pitter, R. L., Hallett, J., and Saunders, C. P. R.: Early electrification and precipitation development in a small, isolated Montana cumulonimbus, *Journal of Geophysical Research: Atmospheres*, 91, 1231–1247, https://doi.org/10.1029/JD091iD01p01231, 1986.

Fan, J. W., Rosenfeld, D., Zhang, Y., Giangrande, S. E., Li, Z., Machado, L. A. T., Martin, S. T., Yang, Y., Wang, J., Artaxo, P., Barbosa, H. M. J., Braga, R. C., Comstock, J. M., Feng, Z., Gao, W., Gomes, H. B., Mei, F., Pöhlker, C., Pöhlker, M. L., Pöschl, U., and de Souza, R. A. F.: Substantial convection and precipitation enhancements by ultrafine aerosol particles, *Science*, 359, 411–418, DOI: 10.1126/science.aan8461, 2018.

Fan, X., Zhang, Y. J., Zheng, D., Zhang, Y., Lyu, W., Liu, H., and Xu, L.: A new method of three-dimensional location for low-frequency electric field detection array, *Journal of Geophysical Research: Atmospheres*, 123, 8792–8812, https://doi.org/10.1029/2017JD028249, 2018.

Goodman, S. J., Buechler, D. E., Wright, P. D., and Rust, W. D.: Lightning and precipitation history of a microburst-producing storm, *Geophysical Research Letters*, 15, 1185–1188, https://doi.org/10.1029/GL015i011p01185, 1988.

Hall, M. P. M., Cherry, S. M., Goddard, J. W. F., and Kennedy, G. R.: Rain drop sizes and rainfall rate measured by dual-polarization radar, *Nature*, 285, 195–198, https://doi.org/10.1038/285195a0, 1980.

Hayashi, S., Umehara, A., Nagumo, N., and Ushio, T.: The relationship between lightning flash

https://doi.org/10.5194/egusphere-2024-907
Preprint. Discussion started: 24 May 2024

rate and ice-related volume derived from dual-polarization radar, *Atmospheric Research*, 248, 105166, https://doi.org/10.1016/j.atmosres.2020.105166, 2021.

Herzegh, P. H., and Jameson, A. R.: Observing Precipitation through Dual-Polarization Radar Measurements, *Bulletin of the American Meteorological Society*, 73, 1365–1376, https://doi.org/10.1175/1520-0477(1992)073<1365:OPTDPR>2.0.CO;2, 1992.

Heymsfield, A. J.: A Comparative Study of the Rates of Development of Potential Graupel and Hail Embryos in High Plains Storms, *Journal of the Atmospheric Sciences*, 39, 2867–2897, https://doi.org/10.1175/1520-0469(1982)039<2867:ACSOTR>2.0.CO;2, 1982.

Huang, H., Zhao, K., Chan, J. C. L., and Hu, D.: Microphysical Characteristics of Extreme-Rainfall Convection over the Pearl River Delta Region, South China from Polarimetric Radar Data during the Pre-summer Rainy Season, *Advances in Atmospheric Sciences*, 40, 874–886, https://doi.org/10.1007/s00376-022-1319-8, 2023.

Hu, J., Rosenfeld, D., Ryzhkov, A., Zrnic, D., Williams, E., Zhang, P., Snyder, J. C., Zhang, R., and Weitz, R.: Polarimetric radar convective cell tracking reveals large sensitivity of cloud precipitation and electrification properties to CCN, *Journal of Geophysical Research: Atmospheres*, 124, 12194–12205, https://doi.org/10.1029/2019JD030857, 2019.

Illingworth, A. J., Goddard, J. W. F., and Cherry, S. M.: Polarization radar studies of precipitation development in convective storms, *Quarterly Journal of the Royal Meteorological Society*, 113, 469–489, https://doi.org/10.1002/qj.49711347604, 1987.

Jameson, A. R., Murphy, M. J. and Krider, E. P.: Multiple-parameter radar observations of isolated Florida thunderstorms during the onset of electrification, *Journal of Applied Meteorology and Climatology*, 35, 343–354, https://doi.org/10.1175/1520-0450(1996)035<0343:MPROOI>2.0.CO;2, 1996.

Kouketsu, T., Uyeda, H., Ohigashi, T., Oue, M., Takeuchi, H., Shinoda, T., Tsuboki, K., Kubo, M., and Muramoto, K.: A Hydrometeor Classification Method for X-Band Polarimetric Radar: Construction and Validation Focusing on Solid Hydrometeors under Moist Environments, *Journal of Atmospheric and Oceanic Technology*, 32, 2052–2074, https://doi.org/10.1175/JTECH-D-14-00124.1, 2015.

Krehbiel, P. R., Brook, M., and McCrory, R. A.: An Analysis of the Charge Structure of Lightning Discharges to Ground, *Journal of Geophysical Research*, 84, 2432–2456, doi:10.1029/JC084iC05p02432, 1979.

Kumjian, M. R.: Principles and applications of dual-polarization weather radar. Part I: Description of the polarimetric radar variables, *Journal of Operational Meteorology*, 1, 226–242, doi:10.15191/nwajom.2013.0119, 2013.

Kumjian, M. R., Khain, A. P., Benmoshe, N., Ilotoviz, E., Ryzhkov, A. V., and Phillips, V. T. J.: The anatomy and physics of ZDR columns: Investigating a polarimetric radar signature with a spectral bin microphysical model, *Journal of Applied Meteorology and Climatology*, 53, 1820–1843, https://doi.org/10.1175/JAMC-D-13-0354.1, 2014.

Kumjian, M. R., and Ryzhkov, A. V.: Polarimetric signatures in supercell thunderstorms, *Journal of Applied Meteorology and Climatology*, 47, 1940–1961, https://doi.org/10.1175/2007JAMC1874.1, 2008.

Laksen, H. R., and Stansbury, E. J.: Association of lightning flashes with precipitation cores extending to height 7 km, *Journal of Atmospheric and Terrestrial Physics*, 36, 1547–1548, https://doi.org/10.1016/0021-9169(74)90232-3, 1974.

Lang, T. J., and Rutledge, S. A.: A Framework for the Statistical Analysis of Large Radar and Lightning Datasets: Results from STEPS 2000, *Monthly Weather Review*, 139, 2536–2551, https://doi.org/10.1175/MWR-D-10-05000.1, 2011.

Latham, J.: The electrification of thunderstorms, *Quarterly Journal of the Royal Meteorological Society*, 107, 277–298, https://doi.org/10.1002/qj.49710745202, 1981.

Li, H., Moisseev, D., and von Lerber, A.: How does riming affect dual-polarization radar observations and snowflake shape? *Journal of Geophysical Research: Atmospheres*, 123, 6070–6081, https://doi.org/10.1029/2017JD028186, 2018.

Lyu, W., Zheng, D., Zhang, Y., Yao, W., Jiang, R., Yuan, S., Liu, D., Lyu, F., Zhu, B., Lu, G., Zhang, Q., Tan, Y., Wang, X., Liu, Y., Chen, S., Chen, L., Li, Q., and Zhang, Y. J.: A Review of Atmospheric Electricity Research in China from 2019 to 2022, *Advances in Atmospheric Sciences*, 40, 1457–1484, https://doi.org/10.1007/s00376-023-2280-x, 2023.

MacGorman, D. R., and Rust, W. D.: The electrical nature of storms, *Oxford University Press*, 422 pp., 1998.

Mai, C., and Du, Y.: Mesoscale moisture transport in determining the location of daytime convection initiations clustered in time and space over southern China, *Journal of*

https://doi.org/10.5194/egusphere-2024-907
Preprint. Discussion started: 24 May 2024

Geophysical Research: Atmospheres, 127, e2021JD036098, https://doi.org/10.1029/2021JD036098, 2022.

Marshall, J. S., and Radhakant, S.: Radar Precipitation Maps as Lightning Indicators, *Journal of Applied Meteorology and Climatology*, 17, 206–212, https://doi.org/10.1175/1520-0450(1978)017<0206:RPMALI>2.0.CO;2, 1978.

Mattos, E. V., Machado, L. A. T., Williams, E. R., and Albrecht, R. I.: Polarimetric radar characteristics of storms with and without lightning activity, *Journal of Geophysical Research: Atmospheres*, 121, 14201–14220, https://doi.org/10.1002/2016JD025142, 2016.

Mattos, E. V., Machado, L. A. T., Williams, E. R., Goodman, S. J., Blakeslee, R. J., and Bailey, J. C.: Electrification life cycle of incipient thunderstorms, *Journal of Geophysical Research: Atmospheres*, 122, 4670–4697, https://doi.org/10.1002/2016JD025772, 2017.

Park, H. S., Ryzhkov, A. V., Zrnić, D. S., and Kim, K.: The Hydrometeor Classification Algorithm for the Polarimetric WSR-88D: Description and Application to an MCS, *Weather and Forecasting*, 24, 730–748, https://doi.org/10.1175/2008WAF2222205.1, 2009.

Pickering, K. E., Bucsela, E., Allen, D., Ring, A., Holzworth, R., and Krotkov, N.: Estimates of lightning NO_x production based on OMI NO_2 observations over the Gulf of Mexico, *Journal of Geophysical Research: Atmospheres*, 121, 8668–8691, https://doi.org/10.1002/2015JD024179, 2016.

Qie, X., Yuan, S., Chen, Z., Wang, D., Liu D., Sun, M., Sun, Z., Srivastava, A., Zhang, H., Lu, J., Xiao, H., Bi, Y., Feng, L., Tian, Y., Xu, Y., Jiang, R., Liu, M., Xiao, X., Duan, S., Su, D., Sun, C., Xu, W., Zhang, Y., Lu, G., Zhang, D., Yin, Y., and Yu, Y.: Understanding the dynamical-microphysical-electrical processes associated with severe thunderstorms over the Beijing metropolitan region, *Science China Earth Sciences*, 64, 10–26. https://doi.org/10.1007/s11430-020-9656-8, 2021.

Ramachandran, R., Detwiler, A., Helsdon, J., Smith, P. L., and Bringi, V. N.: Precipitation development and electrification in Florida thunderstorm cells during Convection and Precipitation/Electrification Project, *Journal of Geophysical Research: Atmospheres*, 101, 1599–1619, https://doi.org/10.1029/95JD02931, 1996.

Reynolds, S. E., and Brook, M.: CORRELATION OF THE INITIAL ELECTRIC FIELD AND THE RADAR ECHO IN THUNDERSTORMS, *Journal of the Atmospheric Sciences*, 13, 376–380, https://doi.org/10.1175/1520-0469(1956)013<0376:COTIEF>2.0.CO;2, 1956.

Reynolds, S. E., Brook, M., and Gourley, M. F.: Thunderstorm charge separation, *Journal of the Atmospheric Sciences*, 14, 426–436, https://doi.org/10.1175/1520-0469(1957)014<0426:TCS>2.0.CO;2, 1957.

Rosenfeld, D.: TRMM observed first direct evidence of smoke from forest fires inhibiting rainfall, *Geophysical Research Letters*, 26, 3105–3108, https://doi.org/10.1029/1999GL006066, 1999.

Rosenfeld, D., Lohmann, U., Raga, G. B., O'Dowd, C. D., Kulmala, M., Fuzzi, S., Reissell, A., and Andreae, M. O.: Flood or drought: How do aerosols affect precipitation? *Science*, 321, 1309–1313, doi:10.1126/science.1160606, 2008.

Ryzhkov, A. V., Zhuravlyov, V. B., and Rybakova, N. A.: Preliminary results of X-band polarization radar studies of clouds and precipitation, *Journal of Atmospheric and Oceanic Technology*, 11, 132–139, https://doi.org/10.1175/1520-0426(1994)011<0132:PROXBP>2.0.CO;2, 1994.

Saunders, C.: Charge Separation Mechanisms in Clouds, *Space Science Reviews*, 137, 335–353, https://doi.org/10.1007/s11214-008-9345-0, 2008.

Saunders, C. P. R., Keith, W. D., and Mitzeva, R. P.: The effect of liquid water on thunderstorm charging, *Journal of Geophysical Research*, 96, 11007–11017, https://doi.org/10.1029/91JD00970, 1991.

Scharfenberg, K. A., Miller, D. J., Schuur, T. J., Schlatter, P. T., Giangrande, S. E., Melnikov, V. M., Burgess, D. W., Andra, D. L., Foster, M. P. Jr., and Krause, J. M.: The Joint Polarization Experiment: Polarimetric Radar in Forecasting and Warning Decision Making, *Weather and Forecasting*, 20, 775–788, https://doi.org/10.1175/WAF881.1, 2005.

Seliga, T. A., and Bringi, V. N.: Potential Use of Radar Differential Reflectivity Measurements at Orthogonal Polarizations for Measuring Precipitation, *Journal of Applied Meteorology and Climatology*, 15, 69–76, https://doi.org/10.1175/1520-0450(1976)015<0069:PUORDR>2.0.CO;2, 1976.

Shi, D., Zheng, D., Zhang, Y., Zhang, Y. J., Huang, Z., and Lyu, W.: Low-frequency E-field Detection Array (LFEDA)-Construction and preliminary results, *Science China Earth Sciences*, 60, 1896–1908, https://doi.org/10.1007/s11430-016-9093-9, 2017.

Smith, P. L., Musil, D. J., Detwiler, A. G., and Ramachandran, R.: Observations of Mixed-Phase

https://doi.org/10.5194/egusphere-2024-907
Preprint. Discussion started: 24 May 2024

Precipitation within a CaPE Thunderstorm, *Journal of Applied Meteorology and Climatology*, 38, 145–155, https://doi.org/10.1175/1520-0450(1999)038<0145:OOMPPW>2.0.CO;2, 1999.

Snyder, J. C., Ryzhkov, A. V., Kumjian, M. R., Khain, A. P., and Picca, J. C.: A ZDR column detection algorithm to examine convective storm updrafts, *Weather and Forecasting*, 30, 1819–1844, https://doi.org/10.1175/WAF-D-15-0068.1, 2015.

Stolzenburg, M., Marshall, T. C., and Krehbiel, P. R.: Initial electrification to the first lightning flash in New Mexico thunderstorms, *Journal of Geophysical Research: Atmospheres*, 120, 11,253–11,276, https://doi.org/10.1002/2015JD023988, 2015.

Stolzenburg, M., Marshall, T. C., and Rust, W. D.: Serial sounding of electric field through a mesoscale convective system, *Journal of Geophysical Research: Atmospheres*, 106, 12371–12380, https://doi.org/10.1029/2001JD900074, 2001.

Stough, S. M., and Carey, L. D.: Observations of anomalous charge structures in supercell thunderstorms in the Southeastern United States, *Journal of Geophysical Research: Atmospheres*, 125, e2020JD033012, https://doi.org/10.1029/2020JD033012, 2020.

Takahashi, T.: Riming electrification as a charge generation mechanism in thunderstorms, *Journal of the Atmospheric Sciences*, 35, 1536–1548, https://doi.org/10.1175/1520-0469(1978)035<1536:REAACG>2.0.CO;2, 1978.

Takahashi, T., Tajiri, T., and Sonoi, Y.: Charges on Graupel and Snow Crystals and the Electrical Structure of Winter Thunderstorms, *Journal of the Atmospheric Sciences*, 56, 1561–1578, https://doi.org/10.1175/1520-0469(1999)056<1561:COGASC>2.0.CO;2, 1999.

Takahashi, T., Sugimoto, S., Kawano, T., and Suzuki, K.: Riming Electrification in Hokuriku Winter Clouds and Comparison with Laboratory Observations, *Journal of the Atmospheric Sciences*, 74, 431–447, https://doi.org/10.1175/JAS-D-16-0154.1, 2017.

Takahashi, T., Sugimoto, S., Kawano, T., and Suzuki, K.: Microphysical structure and lightning initiation in Hokuriku winter clouds, *Journal of Geophysical Research: Atmospheres*, 124, 13156–13181, https://doi.org/10.1029/2018JD030227, 2019.

Tuttle, J. D., Bringi, V. N., Orville, H. D., and Kopp, F. J.: Multiparameter radar study of a microburst: Comparison with model results, *Journal of the Atmospheric Sciences*, 46, 601–620, https://doi.org/10.1175/1520-0469(1989)046<0601:MRSOAM>2.0.CO;2, 1989.

https://doi.org/10.5194/egusphere-2024-907
Preprint. Discussion started: 24 May 2024

Uman, M. A., and Krider, E. P.: Natural and artificially initiated lightning, *Science*, 246, 457–464, doi:10.1126/science.246.4929.457, 1989.

Vincent, B. R., Carey, L. D., Schneider, D., Keeter, K., and Gonski, R.: Using WSR-88D reflectivity data for the prediction of cloud-to-ground lightning: A central North Carolina study, *National Weather Digest*, 27, 35–44, 2003.

Woodard, C. J., Carey, L. D., Petersen, W. A., and Roeder, W. P.: Operational utility of dual-polarization variables in lightning initiation forecasting, *Electronic J. Operational Meteor.*, 13, 79–102, 2012.

Workman, E. J., and Reynolds, S. E.: Electrical activity as related to thunderstorm cell growth, *Bulletin of the American Meteorological Society*, 30, 142–149, https://doi.org/10.1175/1520-0477-30.4.142, 1949.

Wu, C., Liu, L., Wei, M., Xi, B., and Yu, M.: Statistics-based optimization of the polarimetric radar hydrometeor classification algorithm and its application for a squall line in South China, *Advances in Atmospheric sciences*, 35, 296–316, https://doi.org/10.1007/s00376-017-6241-0, 2018.

Zhang, Y., Lyu, W., Chen, S., Zheng, D., Zhang, Y., Yan, X., Chen, L., Dong, W., Dan, J., and Pan, H.: A review of advances in lightning observations during the past decade in Guangdong, China, *Journal of Meteorological Research*, 30, 800–819, https://doi.org/10.1007/s13351-016-6928-7, 2016.

Zhang, Y. J., Yan, M., Sun, A., and Guo, F.: Thunderstorm electricity. *China Meteorological Press*, 384 pp., 2009.

Zhang, Y. J., Sun, A., Yan, M., Guo, F., Qie, X., and Huang, M.: Numerical Simulations of the Effects of Electric Environment on Hail Growth, *Chinese Journal of Geophysics*, 47, 29–37, https://doi.org/10.1002/cjg2.451, 2004.

Zhao, C.: Data for "Microphysical characteristics of the first lightning flash occurrence within isolated warm-season thunderstorms over South China". Figshare. [Dataset]. https://doi.org/10.6084/m9.figshare.22718437.v5, 2024.

Zhao, C., Zhang, Y. J., Zheng, D., Liu, X., Zhang, Y., Fan, X., Yao, W., and Zhang, W.: Using polarimetric radar observations to characterize first echoes of thunderstorms and nonthunderstorms: A comparative study, *Journal of Geophysical Research: Atmospheres*, 127, e2022JD036671, https://doi.org/10.1029/2022JD036671, 2022.

Zhao, C., Zhang, Y. J., Zheng, D., Zhou, Y., Xiao, H., and Zhang, X.: An improved hydrometeor identification method for X-band dual-polarization radar and its application for one summer Hailstorm over Northern China, *Atmospheric Research*, 245, 105075, https://doi.org/10.1016/j.atmosres.2020.105075, 2020.

Zhao, C., Zheng, D., Zhang, Y. J., Liu, X., Zhang, Y., Yao, W., and Zhang, W.: Turbulence Characteristics before the Occurrence of the First Flash in Thunderstorms and Non-Thunderstorms, *Geophysical Research Letters*, 48, e2021GL094821, https://doi.org/10.1029/2021GL094821, 2021a.

Zhao, C., Zheng, D., Zhang, Y. J., Liu, X., Zhang, Y., Yao, W., and Zhang, W.: Characteristics of cloud microphysics at positions with flash initiations and channels in convection and stratiform areas of two squall lines, *Journal of Tropical Meteorology*, 37, 358–369, doi:10.16032/j.issn.1004-4965.2021.035, 2021b.

Zheng, D., Zhang, Y., Zhang, Y., Lyu, W., Chen, L., and Shi, D.: Lightning activity characteristics as indicated by lightning location systems in Guangdong, *in: 1^{st} International Workshop of the Southern China Monsoon Rainfall Experiment (SCMREX), Beijing, China*, 12–13 April, 2017.

Zrnic, D. S., and Ryzhkov, A. V.: Polarimetry for Weather Surveillance Radars, *Bulletin of the American Meteorological Society*, 80, 389–406, https://doi.org/10.1175/1520-0477(1999)080<0389:PFWSR>2.0.CO;2, 1999.

Authors contributions

Conceptualization: C. Zhao, Y. Zhang

Data curation: C. Zhao, Y. Zhang, D. Zheng, S. Du, and X. Liu

Formal analysis: C. Zhao, Y. Zhang, H. Li, X. Peng, P. Zhao, J. Zheng, and J. Shi

Funding acquisition: Y. Zhang, C. Zhao

Investigation: C. Zhao, Y. Zhang

https://doi.org/10.5194/egusphere-2024-907
Preprint. Discussion started: 24 May 2024

Methodology: C. Zhao, Y. Zhang, and H. Li

Project Administration: Y. Zhang

Resources: C. Zhao, Y. Zhang

Software: C. Zhao, D. Zheng

Supervision: Y. Zhang

Validation: C. Zhao, Y. Zhang

Visualization: C. Zhao, Y. Zhang, and H. Li

Writing-original draft: C. Zhao, Y. Zhang, X. Peng, and H. Li

Competing interests

The contact author has declared that none of the authors has any competing interests.